



Relationships between climate change, human environmental impact, and megafaunal extinction inferred from a 4000-year multi-proxy record from a stalagmite from northwestern Madagascar

L. Bruce Railsback ^{a,*}, Laura A. Dupont ^a, Fuyuan Liang ^b, George A. Brook ^c, David A. Burney ^d, Hai Cheng ^{e,f}, R. Lawrence Edwards ^f

^a Department of Geology, University of Georgia, Athens, GA, 30602, USA

^b Department of Geography, Western Illinois University, 1 University Circle, Macomb, IL, 61455, USA

^c Department of Geography, University of Georgia, Athens, GA, 30602, USA

^d National Tropical Botanical Garden, 3530 Papalina Road, Kalaheo, HI, 96741, USA

^e College of Global Environmental Change, Xi'an Jiaotong University, Xi'an, Shaanxi, 710049, China

^f Department of Earth Sciences, University of Minnesota, Minneapolis, MN, 55455, USA



ARTICLE INFO

Article history:

Received 22 January 2020

Received in revised form

24 February 2020

Accepted 25 February 2020

Available online xxx

Keywords:

Africa

Madagascar

Paleoclimatology

Speleothems

Stalagmite

Holocene

Extinction

Landscape

Environment

ABSTRACT

Stalagmite ANJ94-2 from Anjohibe Cave in northwestern Madagascar provides an exceptionally detailed and precisely dated record of changing environmental conditions that, combined with previously published data from stalagmites, wetland deposits, and archaeological sites, allows insights into past climate change, human environmental impact, and megafaunal extinction. Proxies of past conditions recovered from Stalagmite ANJ94-2 include ratios of carbon and oxygen stable isotopes ($\delta^{13}\text{C}$ and $\delta^{18}\text{O}$), mineralogy (calcite and aragonite), layer-bounding surfaces, layer-specific width, and detrital material. Those proxies suggest that the natural environment changed in response to changes in rainfall at time scales of a few decades to multiple centuries; comparison with distant proxies suggests that wetter conditions in northwestern Madagascar may have been linked to cooling in the Northern Hemisphere. Carbon isotope data nonetheless suggest that the greatest environmental change in the area coincided with human introduction of swidden (*tavy*) agriculture about 1200 years ago, during a time not of drought but perhaps of slightly increasing wetness. The timing and extent of environmental change 1200 to 600 years ago seen in stalagmite and wetland data suggest that human modification of the landscape had a causal role in the extinction of Madagascar's megafauna. On the other hand, the results combine with other recent research to indicate that drought was not the cause of the megafaunal extinction.

© 2020 Elsevier Ltd. All rights reserved.

1. Introduction

Madagascar is an island so large and environmentally diverse that it is arguably a small continent (De Wit, 2003), and the title of one book about Madagascar is indeed "The Eighth Continent" (Tyson, 2000). Madagascar's unique history has led at least one author to call it an "alternate world" (Jolly, 1980, p. 10) and other authors to call it "a place of biological wonder" (Yoder and Nowak, 2006). It was apparently not populated by humans until the Holocene (Hansford et al., 2018) and perhaps only for the last two

millennia or less (Mitchell, 2019). The paleoenvironmental history of Madagascar is of great interest because of the extinction of vertebrates, and especially larger vertebrates in the island's "megafauna," in the late Quaternary. The coincidence of so many extinctions with the presence of humans has prompted the hypothesis that humans caused the extinctions, through either predation or landscape modification (e.g., Crowley, 2010; Dewar and Richard, 2012). An alternate hypothesis has been that changing climate, largely in the form of increasingly dry conditions, caused the extinctions (as discussed in further detail by Crowley et al., 2017). The contentious nature of this debate (as analyzed, for example, by Pollini (2010) and Douglass and Zinke (2015)) has led many reviewers to wait for more data, as Dewar and Richard (2012) did with their statement that "a full understanding of the

* Corresponding author. Department of Geology, University of Georgia, Athens, GA, 30602-2501, USA.

E-mail address: rslbk@gyuga.edu (L.B. Railsback).

extinctions will require better evidence and more precise dating".

This article provides some of that "better evidence and more precise dating" in the paleoenvironmental record of Stalagmite ANJ94-2 from Anjohibe Cave in northwestern Madagascar. Stalagmite ANJ94-2 grew from approximately 3.9 ka BP to 250 BP (1700 CE)¹ and thus through the most likely period of human arrival in Madagascar, during the time of megafaunal extinction, and more broadly across multiple ~800-year cycles of wetter and drier climate. Nineteen ²³⁰Th ages with an average uncertainty of ±35 years (and the majority of which have uncertainties of no more than ±12 years) give "precise dating", and 226 measurements of carbon and oxygen stable isotope ratios combine with detailed mineralogic and petrographic observations to provide a robust record of changing conditions to evaluate recent hypotheses about Madagascar's paleoclimatological and paleoenvironmental history.

2. Setting

2.1. General geography

Madagascar is located in the southwestern Indian Ocean and ranges in latitude from 12.0 to 25.6°S, and thus across the Tropic of Capricorn. It is separated from Africa by the Mozambique Channel, which ranges in width from 420 km to 900 km and which reaches depths of more than 3000 m. Madagascar's dominant topographic feature is its Central Highlands, a nearly straight N–S ridge with elevations of 800–1800 m parallel to the length of the island and separating the eastern one-sixth, the eastern coast, from the rest of the island (Fig. 1).

2.2. Climate and vegetation

Because Madagascar lies in the zone of the easterly trade winds (Jury et al., 1995; Jury, 2003), the Central Highlands oriented almost perpendicular to those winds exert a considerable orographic effect on rainfall. In the Köppen-Geiger classification of climate, the coastal region east of the Highlands has a fully humid equatorial (Af) climate, and the Highlands themselves have a fully humid warm temperate climate (Cfa and Cfb) (Kottek et al., 2006; Beck et al., 2018) (Fig. 2). The natural vegetation east of the crest of the Highlands is thus evergreen forest (Du Puy and Moat, 1996).

West of the Highlands and thus in their rain shadow, most of Madagascar has a drier climate, largely in the equatorial dry-winter (Aw) category. As a result, much of central and western Madagascar is covered by grasslands, although the extent to which those grasslands are natural or anthropogenic is hotly debated (Bond et al., 2008; Dewar and Richard, 2012; Quéméré et al., 2012), to the extent that some authors map the region as "dry deciduous forest" that is now "secondary grasslands" (Yoder and Nowak, 2006).

The Inter-Tropical Convergence Zone (ITCZ) migrates southward from the Indian Ocean over northern if not central Madagascar during austral summer (i.e., DJF), bringing rain (Jury and Pathack, 1991; Waliser and Gautier, 1993; Nassor and Jury, 1998; Ziegler et al., 2013) (Fig. 3). The significance of the ITCZ to rainfall in Africa has been questioned (Nicholson, 2018), but the zones of lowest atmospheric pressure and of convergent winds move southward across the Indian Ocean during austral summer and are over

Madagascar during the rainy summers there, indicating that the ITCZ is significant to rainfall east of, and thus free of the modifying effects of, the African continent (Fig. 3).

Austral summer is thus the雨iest season across the entire island, and the season in which tropical cyclones are most frequent (Mavume et al., 2009). This seasonality of rainfall is most extreme in western Madagascar. Across western Madagascar (i.e., in the region of drier rain-shadow climate), rainfall decreases southward from more than 1800 mm/yr in the north to less than 500 mm/yr in the south, presumably with decreasing influence of the ITCZ southward. This pattern has existed in the past, with extreme drying in southwestern Madagascar in the last few thousand years (Burney, 1993a; Virah-Sawmy et al., 2010).

The El Niño – Southern Oscillation phenomenon (ENSO) plays an important but non-uniform role in Madagascar's climate. With regard to temperature, El Niño (i.e., warm wet conditions in the eastern Pacific) is associated with warmer conditions throughout Madagascar and the surrounding ocean (Allan et al., 1996, Fig. 37; Gergis and Fowler, 2009; Fig. 1), and La Niña is associated with cooler conditions. However, teleconnections with regard to precipitation are more restricted geographically. ENSO events like those of 1983 and 1997, which were culturally and/or economically disruptive in many regions, have been associated with drought in southern and central Madagascar (Ingram and Dawson, 2005), and dry conditions in the southwestern two-thirds of Madagascar are generally teleconnected with warm and wet ENSO conditions in the eastern Pacific (Allan et al., 1996; Neelin, 2011; World Meteorological Organization, 2014). In addition, study of corals in the Mozambique Channel off southwest Madagascar confirms a long-term relationship between ENSO and climate there (Zinke et al., 2004). However, no significant relationship to El Niño conditions is observed in northeastern Madagascar. Anjohibe Cave, the focus of this paper, lies on the border between the region of teleconnection and the region with no relationship, suggesting at most a tenuous connection between ENSO and precipitation there.

Another climatic driver in the Indian Ocean and eastern Africa is the Indian Ocean Dipole (IOD) (Saji et al., 1999; Webster et al., 1999). The IOD is an east-west dipole of sea-surface temperature, and with it but lagging a few months in time is a dipole in salinity, the S-IOD (Zhang et al., 2016). However, analysis of climatic records by Scroxton et al. (2017, p. 26) found little relationship between SST anomalies and rainfall in this paper's region of interest in northwestern Madagascar, seemingly because those anomalies are out of phase with the arrival of the ITCZ. Thus both ENSO and IOD, although of great importance to the Indian Ocean in general, seem to have little relationship to rainfall in the region of interest to this paper in northwestern Madagascar.

2.3. Anjohibe Cave

Anjohibe Cave (15.53°S, 46.88°E; ~215 m a.s.l.) is located in northwestern Madagascar about 30 km inland from the Mozambique Channel and about 70 km northeast of Mahajanga or Majunga, the second-largest city of Madagascar. In administrative terms, the cave is in the Mahajanga II district of the Boeny region, which was part of the former Mahajanga province.

The cave is developed in Eocene limestones of the Narinda Karst region (specifically, the Narinda South region of Middleton and Middleton, 2002), and it consists of more than 5 km of mapped passages and thirteen entrances, all in the base of a single hill (Gunn, 2004; Middleton and Middleton, 2002; Voarintsoa et al., 2017a). The cave has been the subject of paleoclimatological study (Brook et al., 1999; Burns et al., 2016; Scroxton et al., 2017; Voarintsoa et al., 2017a, 2017b; 2019; Wang et al., 2019), ecological research (Crowley and Samonds, 2013) and paleoecological

¹ Following the lead of Clarke et al. (2016), this paper uses both BC and BP dates. Clarke et al. (2016) noted that, in the literature, discussion of archaeological data and inferences conventionally uses BC and discussion of paleoenvironmental matters conventionally uses BP. Following the lead of Muigg et al. (2020), this paper uses CE rather than AD for calendrical dates from the present era.

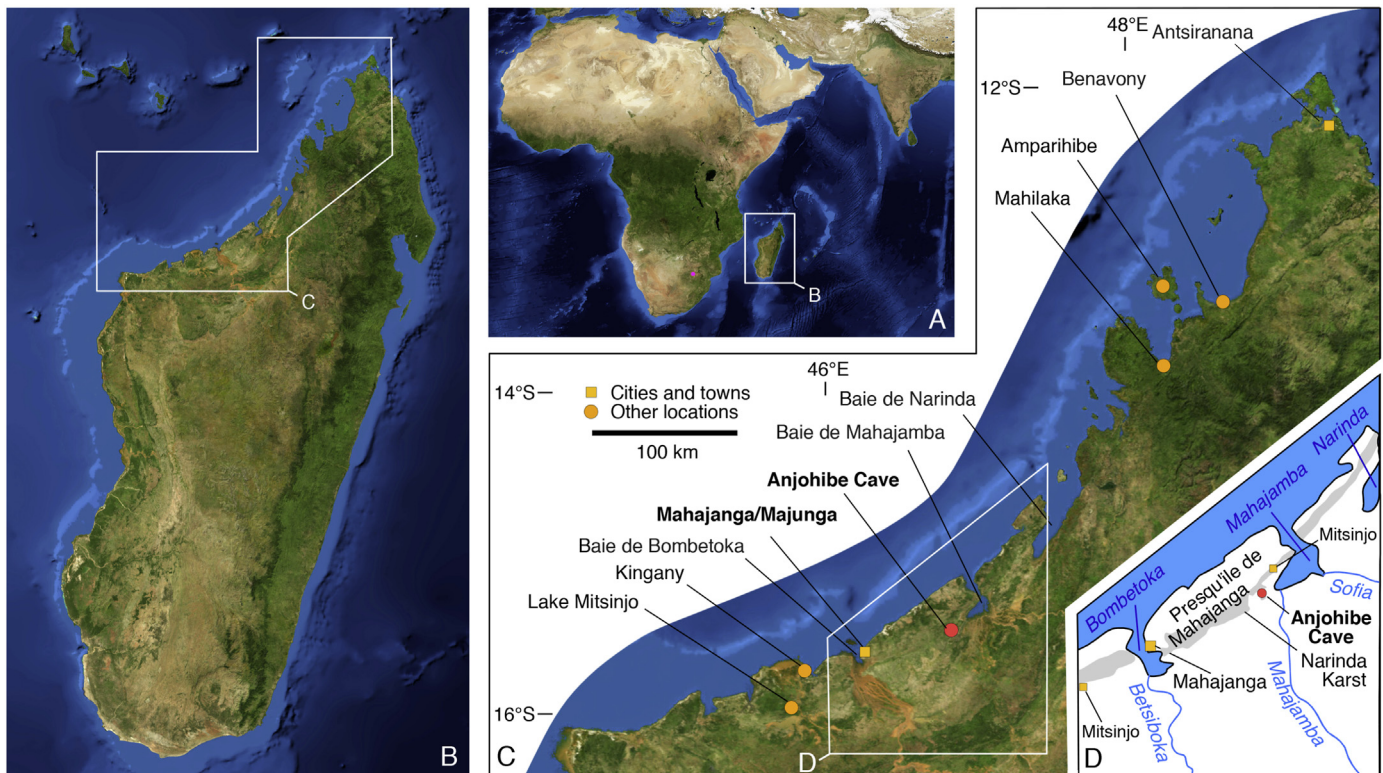


Fig. 1. (A) Image of Africa and the western Indian Ocean. A magenta dot marks the location of Wonderkrater in southern Africa. This image and those in B and C are from the NASA Moderate Resolution Imaging Spectroradiometer (MODIS) program and were obtained in February 2004 as part of the Blue Marble image series. (B) Image of Madagascar. (C) Image of the northwestern coast of Madagascar. Because the image is from the rainy season, rivers are visible and appear red because of their sediment load. The river flowing into the Baie de Bombetoka and thus reaching the coast just west of Mahajanga is the Betsiboka, one of Madagascar's longest rivers. (D) Map of the area of near Anjohibe Cave. There are two towns named Mitsinjo, a larger one west of Mahajanga and north of Lake Mitsinjo and a smaller one east of Mahajanga, near Baie de Mahajamba. According to Middleton and Middleton (2002), both towns have caves named Anjohibe ("Big Cave") nearby; the Anjohibe Cave relevant to this paper is about 10 km southwest of the eastern and smaller Mitsinjo. (For interpretation of the references to colour in this figure legend, the reader is referred to the Web version of this article.)

excavation (e.g., Burney et al., 1997) that have provided many insights about the paleoenvironmental history of northwestern Madagascar. Study of the cave has been sufficiently extensive that it has been proposed as a geopark (Raveloson et al., 2018).

The area around Anjohibe Cave receives 1500–1600 mm of rainfall annually, almost half of which falls in January and February and more than 90% of which falls from November to April as part of the Malagasy or Madagascar Monsoon (e.g., Leroux, 2001). The coolest month is July with a mean of 23.9 °C. The warmest month is November with a mean of 27.8 °C, but the area remains warm until March, when the monthly mean is 27.7 °C.

Anjohibe Cave is in the region of Aw (equatorial dry-winter) climate discussed more generally above, and the landscape over the cave is a savanna with endemic satra palms (*Medemia nobilis*) (Brook et al., 1999; von Cabanis et al., 1969; Wright et al., 1996). A small proportion of the area is dry mesic woodland and forest, but only in areas of high soil moisture (Burns et al., 2016; Voarintsoa et al., 2017a), and Matsumoto and Burney (1994) speculated that grassland with *Medemia nobilis* represents a transition between dry forest and grasslands that are too dry to support any trees at all.

Agriculture in the region typically follows a tradition called "tavy," a form of swidden agriculture. In this system farmers burn their fields and nearby forests in the dry months of September and October to prepare for the onset of the wet season in November (Mittermeier et al., 2008). As a result, more than 80% of the landscape of western Madagascar is now secondary grassland or wooded grassland that is or has been burned each year (Voarintsoa et al., 2017a, and sources cited therein).

3. Materials and methods

3.1. Stalagmite ANJ94-2

Stalagmite ANJ94-2 is approximately 43 cm tall and 8 cm wide with a "fence-post" form externally and with regular symmetrical layers internally, so that it is nearly ideal for paleoenvironmental analysis (Fig. 4). Its upper 36 mm are entirely calcite, the next 48 mm downward are interlayered aragonite and calcite, and the lowest 352 mm are entirely aragonite except for one lamina of calcite that is only 50 µm thick. It was collected in 1994 during fieldwork conducted by Brook and Burney.

3.2. Methods

Twenty-three samples were taken from Stalagmite ANJ94-2 using a dental drill, and care was taken to assure that the samples did not cross layer-bounding surfaces and thus were not diachronous. Those samples were dated using the U-Th or ^{230}Th method, and specifically analyzed using a multi-collector inductively coupled plasma mass spectrometer (MC-ICPMS, Thermo-Finnigan Neptune) in the laboratory of the Department of Earth Sciences of the University of Minnesota. The methods were those described in Shen et al. (2002) and Cheng et al. (2013). The chemical procedure for separation of U and Th was that of Edwards et al. (1987) and Shen et al. (2002). The results were corrected assuming an initial $^{230}\text{Th}/^{232}\text{Th}$ atomic ratio of $4.4 \pm 2.2 \times 10^{-6}$, the value for a material at secular equilibrium with the bulk earth

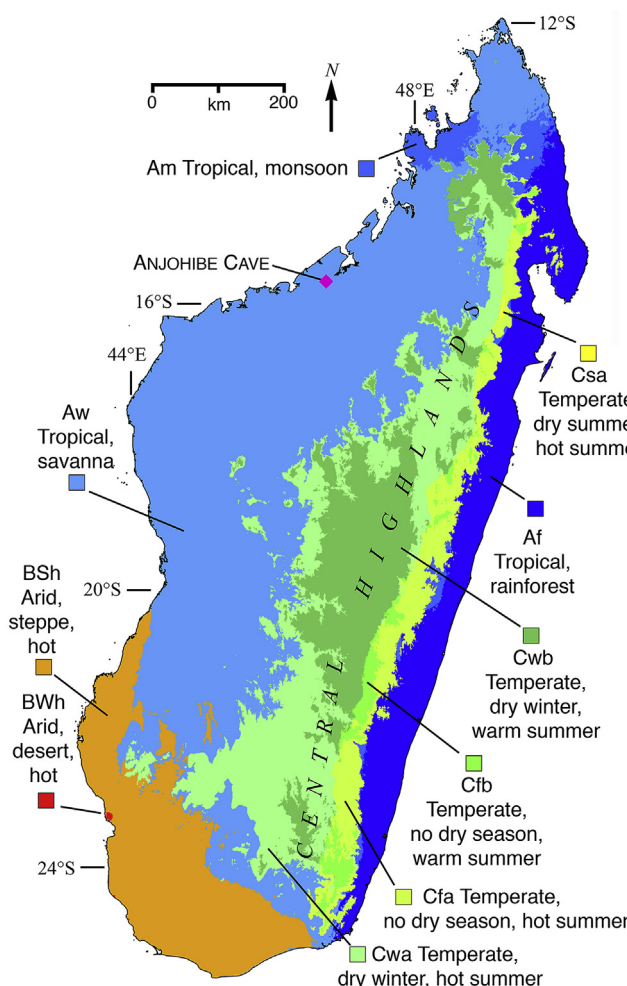


Fig. 2. A map of Köppen-Geiger zones of climate in Madagascar. The pattern shows the interplay of easterly winds, the topography of the Central Highlands, and latitude. Wetter zones are east of the Highlands; west of the Highlands, wetter zones are farther north toward the influence of the ITCZ. The distribution of climate zones portrayed here is from Beck et al. (2018), and the specific map shown here is modified from https://en.wikipedia.org/wiki/File:Koppen-Geiger_Map_MDG_present.svg accessed on January 7, 2020.

$^{232}\text{Th}/^{238}\text{U}$ value of 3.8. Three samples were excluded from construction of the chronology because they had $^{230}\text{Th}/^{232}\text{Th}$ ratios less than 25 and thus age corrections more than 250 years. For the 19 ages used in construction of the chronology, $^{230}\text{Th}/^{232}\text{Th}$ ratios were commonly greater than 1000 and thus corrections were commonly less than 10 years; the largest correction among the ages used was 130 years for each of two replicate samples near the top of the stalagmite. Three ages were rejected because of large uncertainties and because they do not accord with the age trend of other ages with smaller uncertainties; a fourth was rejected because it does not accord with the age trend of other ages.

Stable isotope data ($\delta^{13}\text{C}$ and $\delta^{18}\text{O}$) were collected in two programs of sampling and analysis. For the first program, samples were drilled at intervals of 3–7 mm and designated as “ANJ94-2-*n*”, where *n* is a numeral indicating the place of the sample in a sequence from the top of the stalagmite. These samples were reacted under vacuum with 100% orthophosphoric acid at 50 °C using the methods McCrea (1950) and Al-Aasm et al. (1990). The resulting CO₂ was collected using cryogenic methods and analyzed on a Finnigan-MAT 252 mass spectrometer in the Stable Isotope Laboratory in the Department of Geology of the University of

Georgia. The results were transformed to values of $\delta^{13}\text{C}$ and $\delta^{18}\text{O}$ relative to the VPDB standard using NBS-19 ($\delta^{13}\text{C} = +1.95$, $\delta^{18}\text{O} = -2.2\text{\textperthousand}$ relative to VPDB) and NBS-18 ($\delta^{13}\text{C} = -5.0$ and $\delta^{18}\text{O} = -23.0\text{\textperthousand}$ relative to VPDB). The 2-sigma error of the combined extraction and analysis was 0.04‰ for $\delta^{13}\text{C}$ and 0.05‰ for $\delta^{18}\text{O}$.

For the second program, which focused on segments of enhanced interest, samples were drilled at intervals of 0.3–1.8 mm and designated as “ANJ94-2-L-*n*” where “L” is a letter further indicating a specific segment of the stalagmite. These samples were analyzed using a Delta V Plus mass spectrometer fitted with a GasBench-IRMS machine in the Alabama Stable Isotope Laboratory of the University of Alabama, using the methods and procedures of Paul and Skrzypek (2007), Skrzypek and Paul (2006), and Lambert and Aharon (2011). NBS19 ($\delta^{13}\text{C} = +1.95$, $\delta^{18}\text{O} = -2.2\text{\textperthousand}$ relative to VPDB) and IAEA-603 ($\delta^{13}\text{C} = +2.46$, $\delta^{18}\text{O} = -2.37\text{\textperthousand}$ relative to VPDB) were used as internal standards. The 2-sigma error was approximately $\pm 0.1\text{\textperthousand}$ for both $\delta^{13}\text{C}$ and $\delta^{18}\text{O}$. In both techniques, the results were reported relative to Vienna PeeDee Belemnite (VPDB) and with standardization relative to NBS19.

Data from the second program replaced corresponding samples from the first to give a combined set of 226 measurements of $\delta^{13}\text{C}$ and $\delta^{18}\text{O}$. To correct for fractionation between aragonite and calcite, results from aragonite were transformed to a calcite basis by subtraction of 1.7‰ from $\delta^{13}\text{C}$ values and 0.8‰ from $\delta^{18}\text{O}$ values (Romanek et al., 1992; Kim et al., 2007).

Mineralogy of the stalagmite was determined by thin-section petrography and confirmed by X-ray diffraction using the Bruker D8 X-ray Diffractometer in the Department of Geology of the University of Georgia. Layer-specific width of the stalagmite was determined using a method modified from that of Sletten et al. (2013).

4. Results

4.1. Petrographic observations

Eight layer-bounding surfaces (Railsback et al., 2013) can be identified. These include both Type L surfaces (surfaces below which layers thin and/or are restricted to the center of the stalagmite's crest, suggesting lessened deposition) and Type E surfaces (surfaces at which dissolutional corrosion of the underlying layer is evident, suggesting chemical erosion). The Type L surfaces are all in the lower half of the stalagmite, whereas the Type E surfaces are largely in the upper part of the stalagmite (Fig. 5).

Layer-specific width varies from 17 to 37 mm and is greatest in the upper quarter of the stalagmite. Detrital (non-carbonate) content (as estimated from darkness of the stalagmite and confirmed by thin-section petrography) is likewise greatest in the upper quarter of the stalagmite. If greater layer-specific width is taken as an indication of wetter conditions (Sletten et al., 2013) and Type E surfaces and detrital material are suggestive of wetter conditions (Railsback et al., 2013), these three petrographic indicators suggest wetter conditions largely, but not entirely, later in the stalagmite's growth (Fig. 5). This is in accord with the presence of only calcite in the upper part of stalagmite, because calcite is commonly precipitated in wetter conditions than those in which aragonite forms (Railsback et al., 1994, and sources cited within).

4.2. Chronology

Nineteen ^{230}Th ages (Table 1) combine with the layer-bounding surfaces reported above to give the chronology inferred in Fig. 4. Discontinuities in age and layer-bounding surfaces combine to suggest five hiatuses, two at Type E surfaces and three at each of the

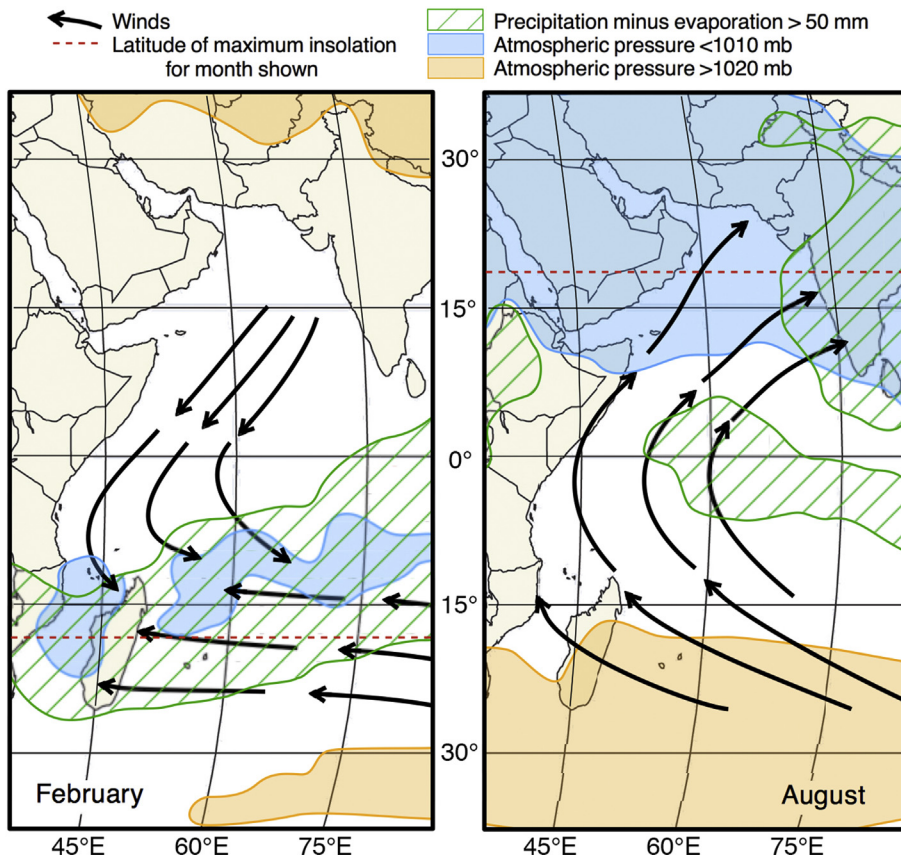


Fig. 3. Maps of the western Indian Ocean showing regions of high and low atmospheric pressure, winds, and regions of positive precipitation minus evaporation (P-E) relevant to the climate of Madagascar. In February (Southern Hemisphere summer), convergence of winds and greatest P-E follow the zone of greatest insolation and lowest atmospheric pressure southward to Madagascar, whereas in August (Southern Hemisphere winter) those regions move far to the north. The maps are derived from maps on the website of Global Climate Animations of the Department of Geography of the University of Oregon at http://geog.uoregon.edu/envchange/clim_animations/index.html. The data come from NCEP/NCAR reanalysis at the Climate Data Center at <http://www.cdc.noaa.gov/cdc/reanalysis>. The underlying map is from the website of Cartographic Research Lab of the Department of Geography of the University of Alabama at <http://alabamamaps.ua.edu/index.html>.

Type L surfaces (at one of which a Type E surface is developed on the Type L surface). The resulting growth rates range from 0.05 mm/yr (during the stalagmite's last 300 years) to 0.26 mm/yr (during a low- $\delta^{13}\text{C}$ low- $\delta^{18}\text{O}$ period at about 3.3 ka BP). Those values are well within the overall range of growth rates of recent stalagmites (Railsback, 2018).

4.3. Stable isotopes

Values of $\delta^{18}\text{O}$, after conversion of values from aragonite to a calcite-basis as noted above, range from -6.4 to $-2.4\text{\textperthousand}$ relative to VPDB. The overall trend of the data is from greater values lower in the stalagmite (and thus earlier) to smaller values higher in the stalagmite (and thus later) (Fig. 5).

Values of $\delta^{13}\text{C}$, likewise after conversion of values from aragonite to a calcite-basis as noted above, vary from -8.6 to $+2.0\text{\textperthousand}$ relative to VPDB and thus yield a range of $10.7\text{\textperthousand}$. That range is uncommonly large for a stalagmite deposited for such a short time, and much of it is due to an exceptional increase of $10.6\text{\textperthousand}$ during the ~350 years from 1148 to 804 BP (802–1146 CE) (Fig. 5).

4.4. Three periods of deposition

The combination of stable isotope data and petrographic observations has led us to divide the history of Stalagmite ANJ94-2 into three periods. The first of these, Period 1, is most of the

stalagmite's time of deposition and extends from the stalagmite's earliest record until 1207 BP (744 CE). It is the period of almost entirely aragonite deposition and includes all three Type L surfaces. It is bounded at its top by a minor Type E surface, by the first sustained deposition of detrital material, and by a spike in $\delta^{13}\text{C}$. Values of $\delta^{13}\text{C}$ and $\delta^{18}\text{O}$ are correlative in Period 1 ($r^2 = 0.62$), $\delta^{13}\text{C}$ values are generally smaller than those in later periods, and $\delta^{18}\text{O}$ values are generally greater than those in later periods.

Period 2, from 1207 to 587 BP (744–1363 CE), was a time of deposition of both calcite and aragonite in which detrital material was consistently included. It includes a Type E surface, and layer-specific width increased during Period 2. Values of $\delta^{13}\text{C}$ increased greatly during Period 2, whereas values of $\delta^{18}\text{O}$ decreased slightly. Values of $\delta^{13}\text{C}$ and $\delta^{18}\text{O}$ are not correlative in Period 2 ($r^2 = 0.02$) (Fig. 6A), but if $\delta^{13}\text{C}$ is detrended with respect to time, values of $\delta^{18}\text{O}$ and detrended $\delta^{13}\text{C}$ are somewhat correlative ($r^2 = 0.42$) (Fig. 6B). The large increase in stalagmite $\delta^{13}\text{C}$ and coeval relative constancy of $\delta^{18}\text{O}$ reported here from Stalagmite ANJ94-2 is replicated in Stalagmite ANJB-2 of Voarintsoa et al. (2017a, b) and Stalagmite ANJ94-5 of Wang et al. (2019), both of which are also from Anjohibe Cave.

Period 3, from 587 BP (1363 CE) to the stalagmite's cessation of growth at 249 BP (1701 CE), was a time of deposition of only calcite, and layer-specific width increased to its greatest value. Values of $\delta^{13}\text{C}$ remained large, and values of $\delta^{18}\text{O}$ decreased further. Values of $\delta^{13}\text{C}$ and $\delta^{18}\text{O}$ are not correlative in Period 3 ($r^2 = 0.03$), and they are

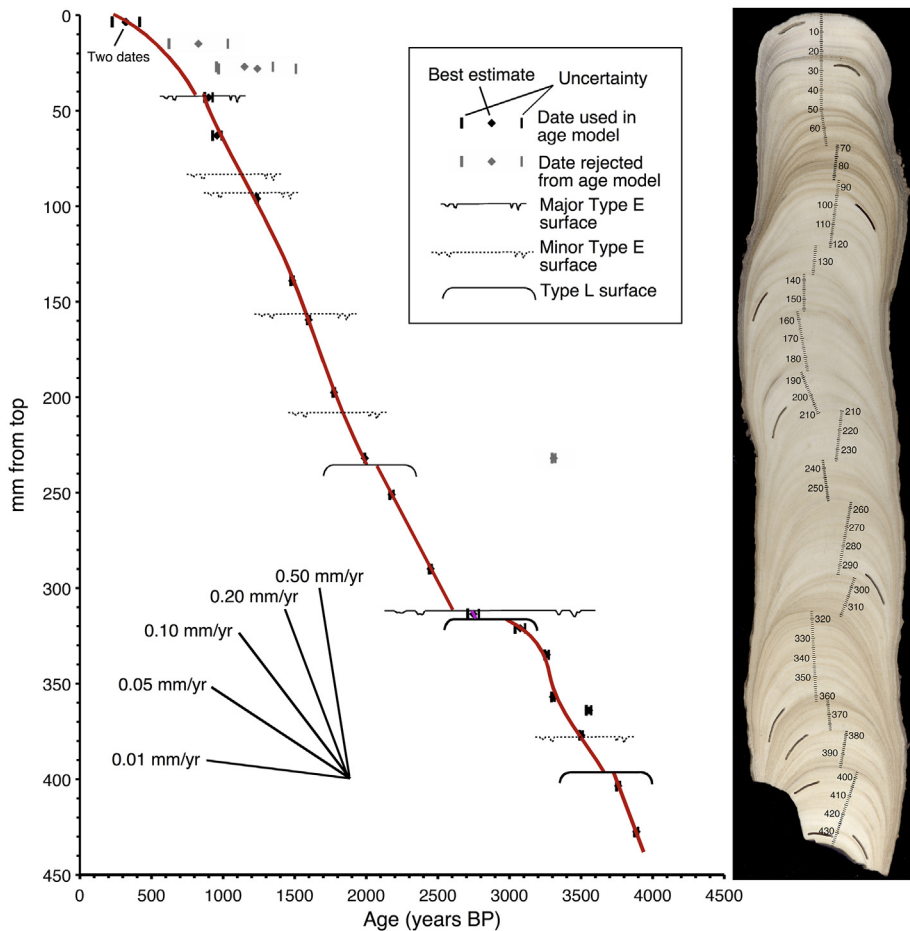


Fig. 4. The age model inferred for Stalagmite ANJ94-2, and an image of the stalagmite with the indexing system superposed. The red curve shows the relationship used to convert positions of samples to ages. The ages and the data from which they were derived are listed in Table 1. Short dark arcs on the stalagmite image are the sampling trenches for some but not all of the ages; the sample from the lowest trench was not analyzed. (For interpretation of the references to colour in this figure legend, the reader is referred to the Web version of this article.)

sufficiently invariant that detrending is irrelevant.

5. Discussion

5.1. Principles guiding interpretation of stable isotope data

Stable isotope data from stalagmites in subtropical regions are commonly interpreted in terms of changes between wetter and drier conditions. With regard to oxygen isotopes, smaller (more negative) values of $\delta^{18}\text{O}$ are commonly attributed to wetter conditions because of an amount effect (McDermott, 2004; Lachniet, 2009), and this concept has been applied in previous work in northern Madagascar (e.g., Burns et al., 2016; Scroxton et al., 2017; Voarintsoa et al., 2017a). That relationship may be strengthened by effects of evaporation (Cuthbert et al., 2014; Markowska et al., 2016; Treble et al., 2017). With regard to carbon isotopes, the most fundamental control is extent of input of ^{13}C -poor carbon by plant-root respiration and organic decay. Thus smaller values of $\delta^{13}\text{C}$ are associated with greater soil biomass and thus greater density of vegetation (e.g., Hesterberg and Siegenthaler, 1991; Lauritzen and Lundberg, 1999; Baldini et al., 2005), which in semi-arid subtropical environments is commonly a function of rainfall. The result is that values of $\delta^{18}\text{O}$ and $\delta^{13}\text{C}$ are commonly correlative in undisturbed subtropical ecosystems (e.g., Fig. 12 of Railsback et al., 2016), whereas decoupling of $\delta^{18}\text{O}$ and $\delta^{13}\text{C}$ is taken as evidence of

unnatural disturbance (e.g., Voarintsoa et al., 2017a, p. 151).

5.2. Paleoceanographical inferences

Most broadly, four if not five proxies ($\delta^{18}\text{O}$, layer-bounding surfaces, layer-specific width, mineralogy, and perhaps detrital content) combine to suggest that Period 1 was a time of generally dry if episodically variable climate, whereas those proxies combine to suggest wetter and perhaps increasing wet climate during Periods 2 and 3 (Fig. 5).

5.2.1. Climate in Period 1

The strong correlation of $\delta^{18}\text{O}$ and $\delta^{13}\text{C}$ in Period 1 suggests a natural undisturbed ecosystem (Figs. 5 and 6). Within Period 1, coincidence of peaks in $\delta^{18}\text{O}$ and $\delta^{13}\text{C}$ with the three Type L surfaces nonetheless suggests episodic climate change in the form of exceptionally dry episodes roughly every 800 years. That periodicity is compatible with reported 800-year cycles in sunspot activity (Nagovitsyn, 2001) and in temperature on the Tibetan Plateau (Liu et al., 2011).

Climate in Period 1 also shows shorter-term and perhaps even more dramatic variability, with sharp swings from exceptionally low to exceptionally high values of both $\delta^{18}\text{O}$ and $\delta^{13}\text{C}$. Two striking examples occurred from 1592 to 1575 BP and from 3275 to 3221 BP; a third possible example occurred from 1150 to 1109 BP in Period 2

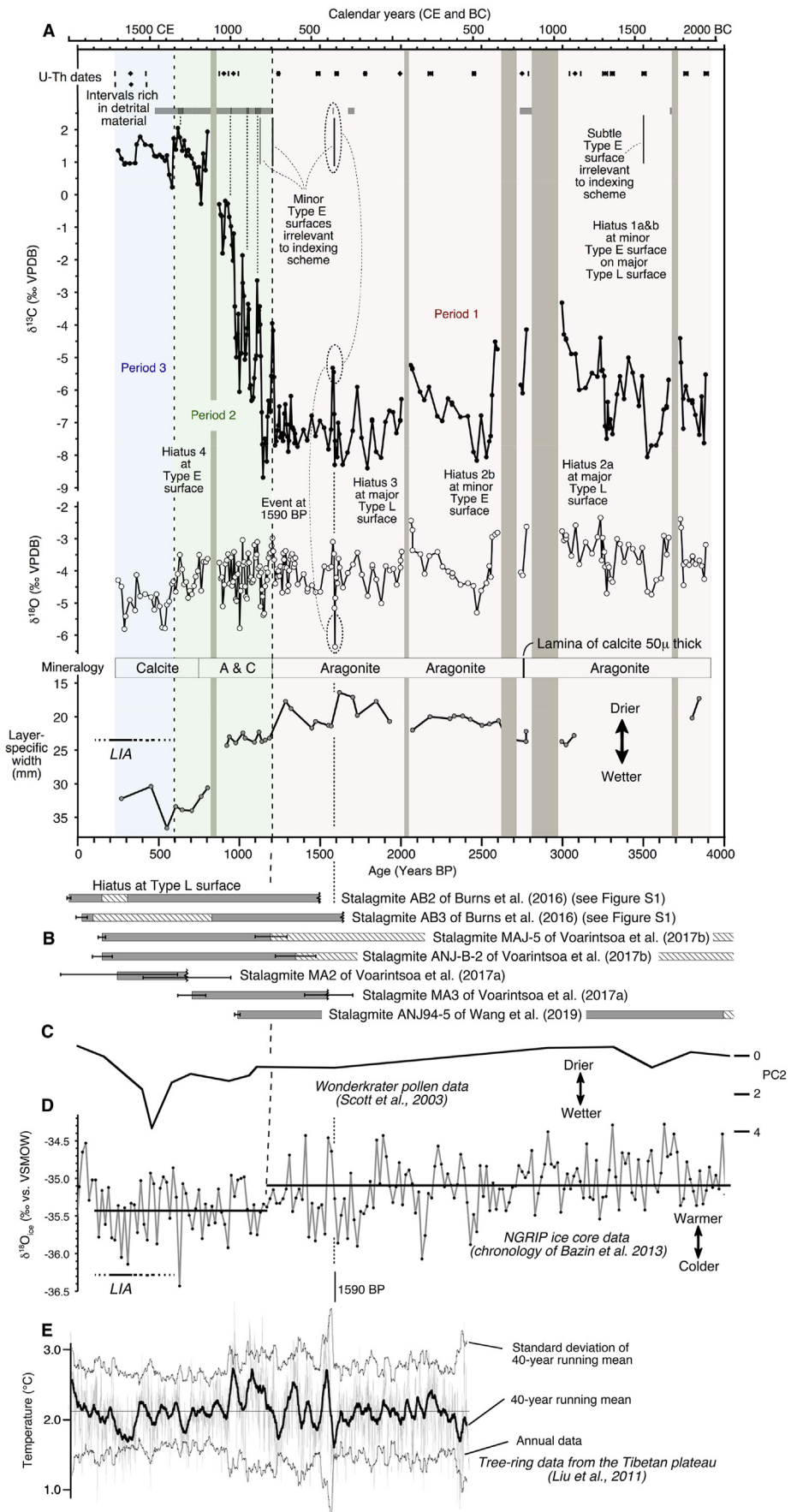


Fig. 5. (A) Isotopic and petrographic data from Stalagmite ANJ94-2 from Anjohibe Cave in northwestern Madagascar; (B) age ranges of other stalagmites from northwestern Madagascar; (C) pollen data from South Africa; (D) ice-core data from Greenland; and (E) a tree-ring record of temperature from the Tibetan Plateau. Fig. 6 examines relationships within the stable isotope data, and Fig. 7 shows time-series of isotopic data during events at 1130 BP, 1580 BP, and 3250 BP in more detail.

(Fig. 7). These isotopic data suggest rapid change from exceptionally wet conditions to exceptionally dry, an inference supported by the presence of a minor Type E surface suggestive of dissolution dating to about 1588 BP (Fig. 5) and thus early in the event from 1592 to 1575 BP. That example is also the most rapid and the most extreme with regard to $\delta^{18}\text{O}$: in about 20 years $\delta^{18}\text{O}$ of stalagmite CaCO₃ changed by 3.3‰, whereas the entire range of $\delta^{18}\text{O}$ for all other samples for Stalagmite ANJ94-2 across its nearly 4000 years is only 3.5‰. All three sharp swings combine to suggest an ecosystem very sensitive to climate change at short time scales, in addition to the longer-term change suggested by the previous paragraph.

5.2.2. Climate in Periods 2 and 3

In contrast to the natural ecosystem inferred for Period 1, the decoupling of $\delta^{18}\text{O}$ and $\delta^{13}\text{C}$ suggests a disturbed ecosystem in

which $\delta^{13}\text{C}$ only secondarily followed climatic controls (Figs. 5 and 6). Nonetheless, decreasing $\delta^{18}\text{O}$, absence of Type L surfaces, greater detrital content, and greater layer-specific width all suggest wetter conditions in Period 2 compared to those of Period 1, and perhaps even wetter in Period 3 (as suggested most strongly by decreasing $\delta^{18}\text{O}$). One might argue that loss of trees with the arrival of agriculture (discussed further below) might lessen evapotranspiration and reduce the residence time for water moving through the soil and karst, causing less evaporation and thus smaller values of $\delta^{18}\text{O}$ than those in earlier times of similar rainfall. However, a similar record may also be seen in the Wonderkrater pollen record of Scott et al. (2003), in that the Wonderkrater results mimic the $\delta^{18}\text{O}$ and layer-specific width trends of ANJ94-2 in suggesting wetter conditions beginning about 1200 BP and reaching greatest wetness around 500 BP (Fig. 5C).

Table 1
 ^{230}Th dating results. The error is 2σ error.

Distance from top (mm)	Sample Number	^{238}U (ppb)	^{232}Th (ppt)	$^{230}\text{Th}/^{232}\text{Th}$ (atomic x10 ⁻⁶)	$\delta^{234}\text{U}^{\text{a}}$ (measured)	$^{230}\text{Th}/^{238}\text{U}$ (activity)	^{230}Th Age (yr) (uncorrected)	^{230}Th Age (yr) ^b (corrected)	$\delta^{234}\text{U}_{\text{Initial}}^{\text{c}}$ (corrected)	^{230}Th Age (yr BP) ^d (corrected)
3.5	ANJ94-2- U002	736 ± 1	3301 ± 66	17 ± 1	0.8 ± 1.7	0.0047 ± 0.0002	514 ± 23	384 ± 95	1 ± 2	320 ± 95
3.5	ANJ94-2- U440	645 ± 1	2884 ± 58	17 ± 1	1.1 ± 1.7	0.0047 ± 0.0003	517 ± 30	387 ± 97	1 ± 2	323 ± 97
15	ANJ94-2- U014	111.1 ± 0.2	1084 ± 22	18 ± 1	2.1 ± 2.1	0.0107 ± 0.0004	1173 ± 49	890 ± 206	2 ± 2	828 ± 206
27	ANJ94-2- U025	196 ± 0	1846 ± 37	24 ± 1	3.0 ± 1.4	0.0136 ± 0.0003	1488 ± 37	1215 ± 197	3 ± 1	1151 ± 197
28	ANJ94-2- U026	71.6 ± 0.1	900 ± 18	20 ± 1	0.5 ± 1.8	0.0152 ± 0.0007	1667 ± 76	1301 ± 270	1 ± 2	1239 ± 270
43	ANJ94-2- U043	2213.2 ± 3.9	2858 ± 57	117 ± 3	2.4 ± 1.5	0.0092 ± 0.0001	1002 ± 9	964 ± 28	2.5 ± 1.5	899 ± 28
63	ANJ94-2- U062	1387.6 ± 2.1	1910 ± 38	116 ± 3	1.1 ± 1.5	0.0097 ± 0.0001	1061 ± 12	1021 ± 31	1 ± 1	959 ± 31
96	ANJ94-2- U093	1965 ± 3	224 ± 5	1728 ± 36	2.9 ± 1.3	0.0119 ± 0.0000	1304 ± 5	1301 ± 6	3 ± 1	1237 ± 6
139	ANJ94-2- U135	2016 ± 3	788 ± 16	601 ± 12	2.8 ± 1.2	0.0142 ± 0.0000	1558 ± 6	1547 ± 10	3 ± 1	1483 ± 10
159.5	ANJ94-2- U160	1470.5 ± 2.3	158 ± 4	2329 ± 53	0.2 ± 1.4	0.0151 ± 0.0001	1663 ± 9	1660 ± 9	0 ± 1	1598 ± 9
197.5	ANJ94-2- U195	1772 ± 2	98 ± 2	5020 ± 118	1.8 ± 1.3	0.0168 ± 0.0001	1840 ± 7	1838 ± 7	2 ± 1	1774 ± 7
232	ANJ94-2- U232	5926.0 ± 12.8	753 ± 15	3967 ± 81	2.0 ± 1.6	0.0306 ± 0.0001	3379 ± 11	3375 ± 11	2.0 ± 1.6	3309 ± 11
232	ANJ94-2- 232.5	2001.0 ± 2.3	216 ± 5	2860 ± 71	0.4 ± 1.3	0.0187 ± 0.0001	2059 ± 12	2056 ± 12	0 ± 1	1989 ± 12
251	ANJ94-2- U245	1283.8 ± 1.9	353 ± 7	1224 ± 26	1.1 ± 1.4	0.0204 ± 0.0001	2247 ± 11	2239 ± 13	1 ± 1	2177 ± 13
290	ANJ94-2- U285	1769 ± 2	259 ± 5	2570 ± 53	1.9 ± 1.1	0.0229 ± 0.0001	2517 ± 8	2513 ± 9	2 ± 1	2449 ± 9
313.5	ANJ94-2- U314	5809.0 ± 10.0	10607 ± 213	235 ± 5	1.3 ± 1.4	0.0260 ± 0.0001	2866 ± 9	2813 ± 39	1.3 ± 1.4	2747 ± 39
321	ANJ94-2- U321	1691.5 ± 3.1	2684 ± 54	300 ± 6	3.2 ± 1.8	0.0289 ± 0.0001	3186 ± 13	3140 ± 35	3.3 ± 1.8	3074 ± 35
335	ANJ94-2- U335	7058.6 ± 15.4	3270 ± 66	1072 ± 22	-1.3 ± 1.4	0.0301 ± 0.0001	3340 ± 11	3326 ± 14	-1.4 ± 1.5	3260 ± 14
357	ANJ94-2- U350	2082 ± 4	218 ± 5	4786 ± 101	0.3 ± 1.5	0.0305 ± 0.0001	3372 ± 10	3369 ± 11	0 ± 2	3305 ± 11
364	ANJ94-2- U364	1538.1 ± 2.2	793 ± 16	1052 ± 22	4.0 ± 1.4	0.0329 ± 0.0001	3635 ± 14	3620 ± 17	4.0 ± 1.4	3554 ± 17
377	ANJ94-2- U372	1813 ± 2	149 ± 3	6468 ± 142	0.4 ± 1.3	0.0322 ± 0.0001	3567 ± 11	3565 ± 11	0 ± 1	3501 ± 11
403.5	ANJ94-2- U408	2124 ± 3	636 ± 13	1906 ± 39	2.0 ± 1.2	0.0346 ± 0.0001	3833 ± 11	382 ± 12	2 ± 1	3760 ± 12
427.5	ANJ94-2- U435	2035 ± 3	164 ± 4	7299 ± 159	2.1 ± 1.2	0.0357 ± 0.0001	3952 ± 11	3950 ± 12	2 ± 1	388 ± 12

^a $\delta^{234}\text{U} = ([^{234}\text{U}/^{238}\text{U}]_{\text{activity}} - 1) \times 1000$.

^b Corrected ^{230}Th ages assume the initial $^{230}\text{Th}/^{232}\text{Th}$ atomic ratio of $4.4 \pm 2.2 \times 10^{-6}$. Those are the values for a material at secular equilibrium, with the bulk earth $^{232}\text{Th}/^{238}\text{U}$ value of 3.8. The errors are arbitrarily assumed to be 50%.

^c $\delta^{234}\text{U}_{\text{Initial}}$ was calculated based on ^{230}Th age (T), i.e., $\delta^{234}\text{U}_{\text{Initial}} = \delta^{234}\text{U}_{\text{measured}} \times e^{\lambda^{234} \times T}$.

^d B.P. stands for "Before Present" where the "Present" is defined as the year 1950 A.D.

Within Period 2, short-lived drier events are evident at intervals of about 80 years, and they give rise to the correlation of $\delta^{18}\text{O}$ with temporally-detrended $\delta^{13}\text{C}$ in Fig. 6B. During the most long-lived of these events, from 960 to 900 BP, Stalagmite ANJ94-5 of Wang et al. (2019) stopped growing after a final increase in $\delta^{13}\text{C}$ of 5.5‰.

5.2.3. Teleconnections and larger-scale patterns

Relationships between the ANJ94-2 record and other paleoclimatological records allow evaluation of three hypotheses. Hypothesis I is that shifts of the ITCZ from a cooling hemisphere or to a warming hemisphere (Broccoli et al., 2006; Kang et al., 2008; Donohoe et al., 2013) have driven climate change in Madagascar, with cooler global climate expressed more in the Northern Hemisphere bringing wetter conditions to Madagascar. Hypothesis II is that weakening of the AMOC and associated lessening of Agulhas Leakage (i.e., reduced passage of warm water from the Indian to the South Atlantic, as suggested by Fig. 1 of Railsback (2019), which draws on Richardson (2007)) have brought more rain to northern Madagascar during cool phases in the Northern Hemisphere. Hypothesis III is that lessening of the width of the ITCZ latitudinal migration has caused drier conditions in Madagascar during globally cool phases (Singarayer et al., 2017). The increase in wetness in northwestern Madagascar inferred at the beginning of Period 2 (at 1.21 ka BP) coincides with one of the largest decreases of $\delta^{18}\text{O}$ in the NGRIP record of Bazin et al. (2013), at 1.17 ka BP. This coincidence of increasing rainfall in northwestern Madagascar with apparent cooling in the North Atlantic would be consistent with Hypotheses I and II but not Hypothesis III. The further increase of wetness inferred in northwest Madagascar at the beginning of Period 3 at 1.36 ka (but in the least precisely dated period of ANJ94-2) coincides roughly with the beginning of the Little Ice Age, when at least some stalagmite records from southern Africa also indicate wetter conditions (Voarintsoa et al., 2016; Railsback et al., 2018). This too would be consistent with Hypotheses I and II but not Hypothesis III. Hypotheses I and II are, of course, not mutually exclusive, but the conclusions of Scroxton et al. (2017) and Wang et al. (2019) are more in accord with Hypothesis II, in that changes in northwest Madagascar may have been in-phase, rather than antiphase, with changes in northern-hemisphere regions in the northern Indian Ocean and eastern Africa.

With those general observations made with regard to Periods 2 and 3, one can focus at higher resolution on the earlier abrupt and large swing from strikingly low values of $\delta^{18}\text{O}$ and $\delta^{13}\text{C}$ to strikingly high ones around 1590 BP (Figs. 5 and 7). This abrupt shift coincides with the largest change in a 2500-year tree-ring record from the Himalayan Plateau (Liu et al., 2011), an abrupt swing from exceptionally cold conditions to exceptionally warm ones. This much shorter-term event, like the longer-term shifts discussed in the previous paragraph, would suggest linkage of cooler conditions in the Northern Hemisphere (but outside the Atlantic) with wetter conditions in northwestern Madagascar and thus be compatible with a model of ITCZ migration toward the warmer hemisphere, and thus with Hypothesis I.

5.3. Landscape disturbance and human activity

The observed decoupling of $\delta^{13}\text{C}$ from $\delta^{18}\text{O}$ and increase in detrital content in Period 2 suggest major disturbance of the overlying landscape. The abrupt and large (>10‰) increase in stalagmite $\delta^{13}\text{C}$ in ANJ94-2 (and in its two compatriots ANJB-2 of Voarintsoa et al. (2017b) and Stalagmite ANJ94-5 of Wang et al. (2019)) suggests drastic lessening of vegetation and soil biomass, and the increase in detrital content of the stalagmite suggests a landscape destabilized by loss of vegetation. Some part of the overall increase in stalagmite $\delta^{13}\text{C}$ may be the result of a transition

from a native C₃-dominant dry forest to the present C₄-dominant palm savanna, as suggested by $\delta^{13}\text{C}$ data from both stalagmites (Burns et al., 2016) and bones from Anjohibe Cave (Crowley and Samonds, 2013). However, the magnitude of the increase in $\delta^{13}\text{C}$ in Stalagmite ANJ94-2 requires drivers beyond the scale of the difference in photosynthetic mechanisms, which typically cause changes in $\delta^{13}\text{C}$ of ~4‰ (Dorale et al., 1992; Denniston et al., 1999; Zhu et al., 2006). Instead, the observed change in $\delta^{13}\text{C}$ of ~10‰ suggests a major reduction, or an accompanying major reduction, in the quantity of vegetation (Jiménez de Cisneros and Caballero, 2011).

The timing of this landscape disturbance coincides with other indicators of alteration of the landscape in northwestern Madagascar. For example, concentration of charcoal in sediments from lakes (Mitsinjo and Amparihibe) and marshes (Benavony) along Madagascar's northwest coast increased dramatically at about 1200 BP (Fig. 8D). At about the same time, the proportion of grass pollen in Lake Mitsinjo sediments southwest of Anjohibe Cave increased (Matsumoto and Burney (1994), as summarized by Wright et al. (1996)) (Fig. 8). The period from 1300 to 1200 BP also marks a spike in extinction of endemic chordate genera (Crowley,

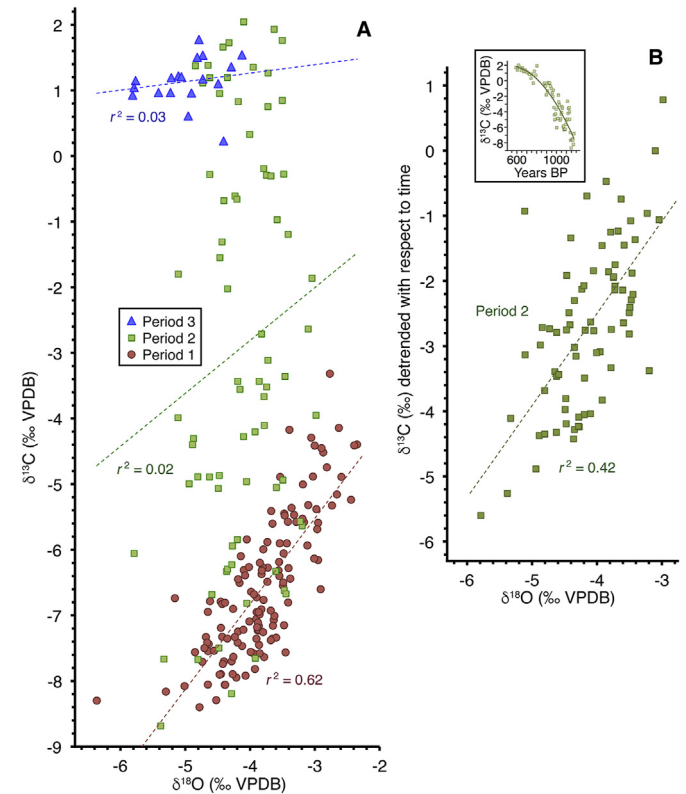


Fig. 6. Plots of variation of $\delta^{13}\text{C}$ with respect to $\delta^{18}\text{O}$ in data from Stalagmite ANJ94-2. (A) Plot of data from Periods 1, 2, and 3. The strong correlation of data from Period 1 is consistent with climatic control on both $\delta^{13}\text{C}$ and $\delta^{18}\text{O}$. (B) Plot of $\delta^{13}\text{C}$ data from Period 2 after detrending with respect to time. The inset shows the original $\delta^{13}\text{C}$ data plotted with respect to time (as in Fig. 5) and the curve resulting from second-order regression of those data with respect to time. To construct the main plot of Part B, detrending with respect to time (t in years BP) of each original $\delta^{13}\text{C}$ value was accomplished by subtracting the corresponding value on the curve. ($\delta^{13}\text{C}_{\text{curve}} = -0.0000133xt^2 + 0.0082xt + 1.9877$) and adding the result to the mean of the original $\delta^{13}\text{C}$ values for Period 2, which is $-2.7\text{\textperthousand}$. Part B documents that, although raw $\delta^{13}\text{C}$ values show little relationship to $\delta^{18}\text{O}$ in Part A because of a time-dependent shift of overall $\delta^{13}\text{C}$, individual $\delta^{13}\text{C}$ values have a relationship to $\delta^{18}\text{O}$ that suggests continued but only partial dependence on climate. An analogous analysis of data from Period 3 was not performed because the original $\delta^{13}\text{C}$ values from Period 3 show no single or simple trend with time (Fig. 5).

2010), which does not require landscape disruption but suggests some major ecological change.

This ecological disruption was coeval with human activity in northwestern Madagascar. Shards of ceramics dating to 1050 ± 80 BP have been found at Kingany, about 110 km west of Anjohibe Cave, and evidence of cultivation of Asian crops has been found at Mahilaka, about 240 km to the northeast (Crowther et al., 2016). More broadly, although there are recent reports (Hansford et al., 2018) of evidence for humans in Madagascar as long ago as 10.5 ka BP, Mitchell (2019) has argued that evaluation by strict criteria suggests that there is no convincing evidence of humans in Madagascar before about 1500 BP. Coincidence in time is not proof of cause, but the arrival or spread of people who in more recent times have practiced *tavy*, a form of swidden agriculture in which vegetation is removed by burning (as discussed by Voarintsoa et al., 2017a), provides a likely explanation for disturbance of vegetation and an abrupt increase in the concentration of charcoal in sediments. Similarly, Godfrey et al. (2019) reviewed the paleoecological evidence for human impacts on Madagascar and proposed that it was a transition in human land-use, and not human arrival, that has generated a strong signal for human impact beginning about this time. Their proposed "Subsistence Shift Hypothesis" acknowledges the potential importance of animal hunting by early foragers, but highlights the negative impacts of the inferred shift from hunting/foraging to herding/farming by new immigrant groups and the concomitant expansion of the island's human population between ca. 700–900 CE.

5.4. Megafaunal extinction

The causes of the Holocene extinction of Madagascar's megafauna have long been the subject of debate (e.g., Burney et al., 1997), and the extinction has been attributed to many factors ranging from the natural, such as drought (e.g. (Virah-Sawmy et al., 2010), to the human-induced, such as hunting, fire, introduction of competitors, introduction of disease, or general environmental impact (as summarized by Burney et al. (1997) and Burney (1999, p. 147)).

In the last decade, further research has led to greater emphasis on the human role, both direct and indirect, in modifying the environment and thereby inducing extinction (e.g., Crowley, 2010; Dewar and Richard, 2012; Crowley et al., 2017). However, paleo-environmental researchers focusing on longer time scales have argued that Madagascar's fauna had survived environmental change in the form of wildfires, vegetation changes, and climate changes for millennia before the arrival of humans (e.g., Burney, 1993b, p. 539; Quémére et al., 2013; Wang et al., 2019).

The relatively long but detailed record from Stalagmite ANJ94-2 allows insight regarding the cause of the megafaunal extinction. The record's length, extending back nearly 4000 years, allows the observation that, although the environment had undergone major environmental change recorded most obviously by changes in $\delta^{13}\text{C}$ but also by changes in $\delta^{18}\text{O}$ and by hiatuses in deposition, most megafaunal extinctions were more recent. Wang et al. (2019) observed from Stalagmite ANJ94-5 that rapid changes in climate and major droughts did not exterminate Madagascar's megafauna during the early and middle Holocene, and the ANJ94-2 record extends that thought through much of the later Holocene as well. Instead, most of the megafaunal extinctions coincide with the extreme change in Stalagmite ANJ94-2's $\delta^{13}\text{C}$ (but not $\delta^{18}\text{O}$) record when humans were unquestionably on Madagascar (Mitchell, 2019) and leaving evidence of their presence in the northwest part of the island (Wright et al., 1996; Crowther et al., 2016). The detail of the record also allows close correlation in time of disturbance on the surface above Anjohibe Cave with other indicators of human disruption of the ecosystem (e.g., the large increase in abundance of charcoal in lake and marsh sediments in the region documented by Burney, 1999). The coincidence in time of this disruption (Fig. 8D to G) with the main pulse of megafaunal extinction (Fig. 8C) suggests that the extinction was linked to human activity, at least by disruption of vegetation and landscape with the onset of swidden agriculture, as proposed in Godfrey et al. (2019).

The O isotope record from Stalagmite ANJ94-2 helps lay aside the hypothesis that drought induced the megafaunal extinction.

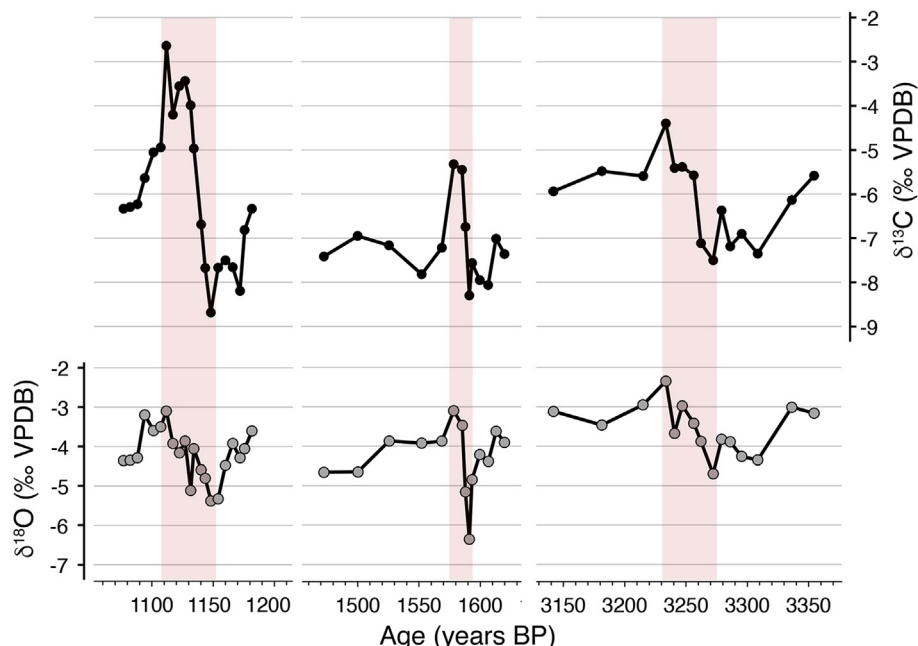


Fig. 7. Plots of C and O stable isotope data in periods with sharp swings from exceptionally low to exceptionally high values of both $\delta^{18}\text{O}$ and $\delta^{13}\text{C}$. Note that the event from 1592 to 1575 BP has the greatest increase of $\delta^{18}\text{O}$ and is the most rapid.

The steadiness or slight decrease in $\delta^{18}\text{O}$ of stalagmite CaCO₃ in ANJ94-2 during the most recent 1200 years (and the renewed growth of Stalagmites MAJ-5 and ANH-B-2) does not support the idea of drought, in accord with the findings of Godfrey et al. (2015), Burns et al. (2016), and Crowley et al. (2017) that drought was not a

factor. Furthermore, Crowley (2010) defined two pulses of megafaunal extinction, with the first from ~2500 to 2000 BP when the ANJ94-2 record shows wetter conditions, supporting the contention that droughts did not cause extinctions.

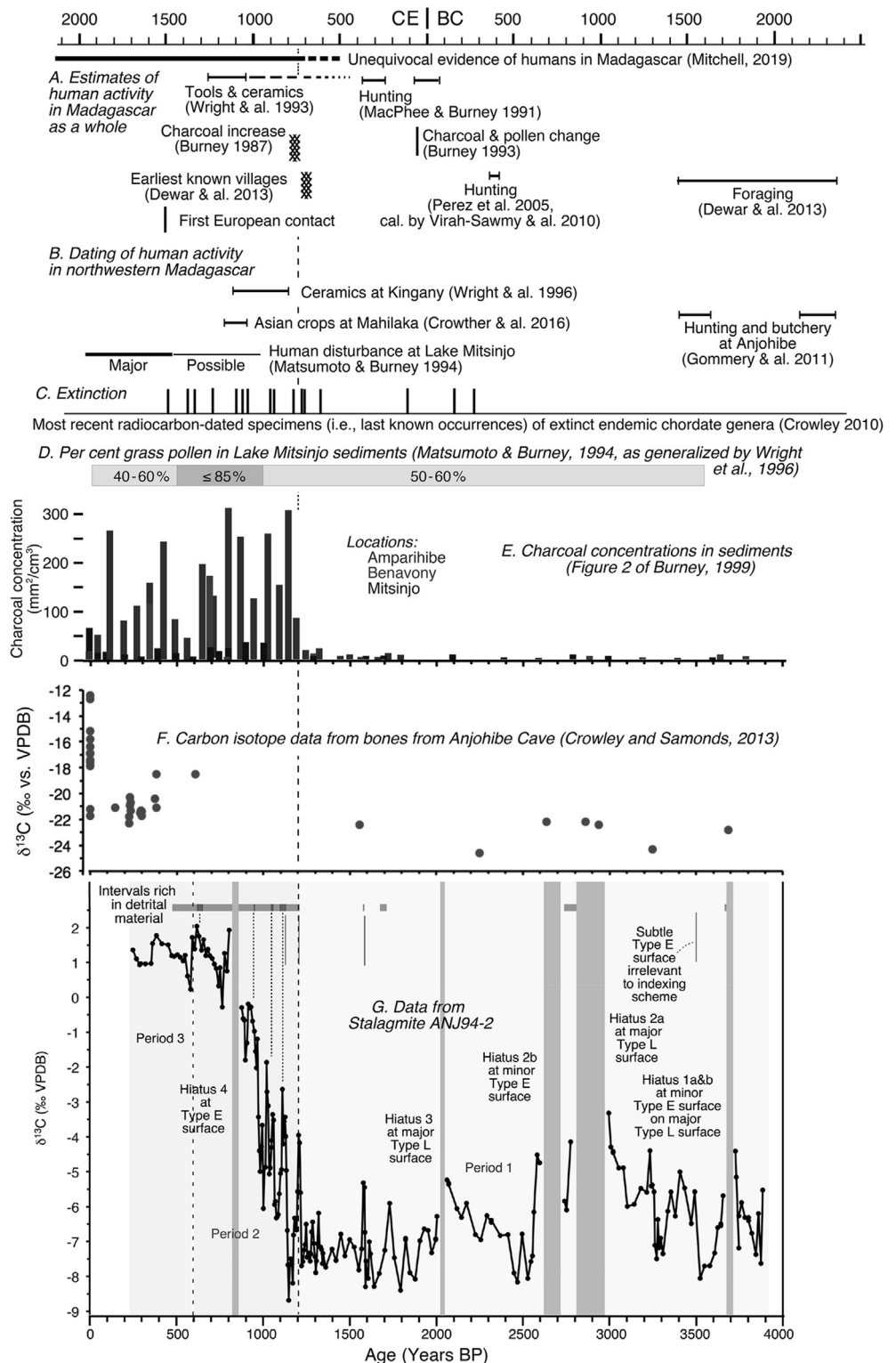


Fig. 8. (A and B) Timing of archaeological evidence in Madagascar; (C to F) data regarding ecosystem change in Madagascar; and (G) carbon isotope data from Stalagmite ANJ94-2. Dashed vertical line shows relationship of stalagmite evidence of landscape disruption to other indicators (Burney, 1987; Dewar et al., 2013; Gommery et al., 2011; MacPhee and Burney, 1991; Perez et al., 2005; Wright et al., 1993).

5.5. The Type E surface dating to ~820 BP: evidence for an alternate origin of type E surfaces?

Sections 5.2 to 5.4 present the principal paleoenvironmental inferences made from this research, and they prompt some reconsideration of the environmental significance of Type E surfaces in stalagmites. Type E surfaces are layer-bounding surfaces at which there is evidence of dissolution, either at microscopic scale as “micromesas” suggesting partial removal of individual layers or at larger scale as layers present on the flanks of the stalagmite but eroded from the crest (Railsback et al., 2013). Railsback et al. (2013) inferred that Type E surfaces are evidence of dissolution and, especially when capped by detrital material, probably result from more rapid passage of water across the stalagmite and thus likely represent wetter conditions in which dripping water passed through the soil too quickly to be charged with CO₂ or gushed onto the stalagmite too quickly to allow degassing of CO₂ and the water's customary saturation or supersaturation with regard to solid CaCO₃. The Type E surface 43 mm from the top of Stalagmite ANJ94-2 that dates to ~820 BP has a morphology unexceptional compared to those of Type E surfaces in other stalagmites, but its context suggests an alternate cause for dissolution, one in which an unexceptional flux of water through the regolith is not charged with CO₂ because the plant community is greatly reduced and/or soil organic matter greatly depleted, in this case by fire in swidden agriculture (but as might happen with any case of extreme erosion). In this scenario, water would reach the stalagmite in much the same state as rainwater falling on bare limestone, where dissolution by similarly unmodified rainwater can result in non-microscopic erosional features like karren (Field, 2002). Because the Type E surface 43 mm from the top of Stalagmite ANJ94-2 is found above an interval of radically increasing δ¹³C and followed immediately by δ¹³C of nearly 2‰ relative to VPDB, it may be an example of a Type E surface that resulted not from wetter conditions but from extreme disruption of the biological system on and in the overlying soil and regolith.

An alternate view not relevant to the Type E surface at 43 mm from the top of Stalagmite ANJ94-2 but perhaps to other stalagmites is that a minor Type E surface might form under generally dry conditions when sudden heavy rains nonetheless occur and water may flow rapidly into fractures to give conduit flow (as opposed to diffuse recharge) to the underlying limestone. Conduit flow would allow the water to drain into the limestone so quickly that it would not reach saturation with respect to calcite, briefly inducing dissolution. This alternate case and that proposed in the previous paragraph both depend on presence of a diminished plant community, this one due to long-term dry climate and that of the previous paragraph to landscape disturbance.

6. Conclusions

The multi-proxy record of Stalagmite ANJ94-2 from Anjohibe Cave in northwestern Madagascar suggests that the natural environment was sensitive to changes in rainfall at time scales of a few decades to multiple centuries. A natural rather than human-modified ecosystem prevailed until about 1200 BP (750 CE). Changes to wetter conditions thereafter may have been linked to cooling in the Northern Hemisphere. However, δ¹³C data suggest that the greatest environmental change coincided with human introduction of swidden agriculture about 1200 years ago, during a time not characterized by drought but perhaps slightly increasing wetness. The timing and extent of environmental change 1200 to 600 years ago suggests that human modification of the environment had some causal role in the extinction of Madagascar's megafauna. At larger geographic scale, consideration of

teleconnections suggests that cooling of the Northern Hemisphere coincided with shifts of the ITCZ southward and/or with weakening of the AMOC and associated lessening of Agulhas Leakage, in either case bringing more rainfall to northwestern Madagascar. On the other hand, patterns in northwestern Madagascar have not been consistent with changing latitudinal width of the ITCZ.

Author statement

All of the authors have made substantial contributions to the submission: Brook and Burney collected the stalagmite and did the field research; Liang, Cheng, and Edwards generated the radiometric ages; Railsback made the layer-specific-width measurements; Railsback and Dupont took samples for stable isotope analysis and generated the interpretation; Railsback revised after review and Dupont and Brook edited that revision. All of the authors have approved the final version of the manuscript.

Declaration of competing interest

The authors declare that they have no known competing financial interests or personal relationships that could have appeared to influence the work reported in this paper.

Acknowledgments

Funding for this research came from U.S. National Oceanic and Atmospheric Administration (NOAA) grant NA56GP0325 to Brook, Railsback, Jean-Claude Thill and Richard S. Meltzer; from US National Science Foundation (NSF) grants 8912046 to Brook, Burney and James B. Cowart, and 9908415 to Brook and Railsback; from National Natural Science Foundation of China (NSFC) grant 41888101 to Cheng; from the Department of Geology of the University of Georgia (USA) in support of an undergraduate thesis by Dupont; and from Prof. Celeste M. Condit. The government and people of Madagascar kindly assisted in making this research possible. Fieldwork in Madagascar was carried out under the auspices of the Cenozoic Research Group, a Malagasy-American collaboration sanctioned by the Service de Paléontologie and the Musée d'Art et d'Archéologie of the Université d'Antananarivo.

References

- Al-Aasm, I.S., Taylor, B.E., South, B., 1990. Stable isotope analysis of multiple carbonate samples using selective acid extraction. *Chem. Geol.* 80, 119–125.
- Allan, R., Lindesay, J., Parker, D., 1996. *El Niño Southern Oscillation & Climatic Variability*. CSIRO Publishing, Collingwood, Australia.
- Baldini, J.U.L., McDermott, F., Baker, A., Baldini, L.M., Mathey, D.P., Railsback, L.B., 2005. Biomass effects on stalagmite growth and isotope ratios: a 20th century analogue from Wiltshire, England. *Earth Planet Sci. Lett.* 240, 486–494.
- Bazin, L., Landais, A., Lemieux-Dudon, B., Toyé Mahamadou Kele, H., Veres, D., Parrenin, F., Martinerie, P., Ritz, C., Capron, E., Lipenkov, V.Y., Loutre, M.F., Raynaud, D., Vinther, B.M., Svensson, A.M., Rasmussen, S.O., Severi, M., Blunier, T., Leuenberger, M.C., Fischer, H., Masson-Delmotte, V., Chappellaz, J.A., Wolff, E.W., 2013. Delta ¹⁸O Measured on Ice Core NGRIP on AICC2012 Chronology. PANGAEA. <https://doi.org/10.1594/PANGAEA.824889>.
- Beck, H.E., Zimmerman, N.E., McVicar, T.R., Vergopolan, N., Berg, A., Wood, E.F., 2018. Present and future Köppen-Geiger climate classification maps at 1-km resolution. *Sci. Data* 5, 180214.
- Bond, W.J., Silander Jr., J.A., Ranaivonasy, J., Ratsirarson, J., 2008. The antiquity of Madagascar's grasslands and the rise of C4 grassy biomes. *J. Biogeogr.* 35, 1743–1758.
- Broccoli, A.J., Dahl, K.A., Stouffer, R.J., 2006. Response of the ITCZ to northern hemisphere cooling. *Geophys. Res. Lett.* 33, L01702. <https://doi.org/10.1029/2005GL024546>.
- Brook, G.A., Rafter, M.A., Railsback, L.B., Sheen, S.-W., Lundberg, J., 1999. A high-resolution proxy record of rainfall and ENSO since AD 1550 from layering in stalagmites from Anjohibe Cave, Madagascar. *Holocene* 9, 695–705.
- Burney, D.A., 1987. Late Holocene vegetational change in central Madagascar. *Quat. Res.* 28, 1300–143.
- Burney, D.A., 1993a. Late Holocene environmental changes in arid southwestern

- Madagascar. *Quat. Res.* 40 (1), 98–106.
- Burney, D.A., 1993b. Recent animal extinctions: recipes for disaster. *Am. Sci.* 81, 529–541.
- Burney, D.A., 1999. Rates, patterns, and processes of landscape transformation and extinction in Madagascar. In: MacPhee, R.D.E. (Ed.), *Extinctions in Near Time – Causes, Contexts, and Consequences*. Kluwer Academic/Plenum Publishers, New York, pp. 145–164.
- Burney, D.A., James, H.F., Grady, F.V., Rafamantanantsoa, J.G., Ramilisonina Wright, H.T., Cowart, J.B., 1997. Environmental change, extinction and human activity: evidence from caves in NW Madagascar. *J. Biogeogr.* 24 (6), 755–767.
- Burns, S.J., Godfrey, L.R., Faina, P., McGee, D., Hardt, B., Ranivoarimanana, L., Randrianasny, J., 2016. Rapid human-induced landscape transformation in Madagascar at the end of the first millennium of the Common Era. *Quat. Sci. Rev.* 134, 92–99.
- Cheng, H., Edwards, R.L., Shen, C.-C., Woodhead, J., Hellstrom, J., Wang, Y.J., Kong, X.G., Spötl, C., Wang, X.F., Alexander Jr., E.C., 2013. Improvements in 230Th dating, 230Th and 234U half-life values, and U-Th isotopic measurements by multi-collector inductively coupled plasma mass spectrometry. *Earth Planet Sci. Lett.* 371–372, 82–91.
- Clarke, J., Brooks, N., Binning, E.B., Bar-Matthews, M., Campbell, S., Clare, L., Cremaschi, M., di Lerna, S., Drake, N., Gallinaro, M., Manning, S., Nicoll, K., Philio, G., Rosen, S., Schoop, U.-D., Tafuri, M.A., Weninger, B., Zerboni, A., 2016. Climatic changes and social transformations in the Near East and North Africa during the 'long' 4th millennium BC: a comparative study of environmental and archaeological evidence. *Quat. Sci. Rev.* 136, 96–121.
- Crowley, B.E., 2010. A refined chronology of prehistoric Madagascar and the demise of the megafauna. *Quat. Sci. Rev.* 29, 2591–2603.
- Crowley, B.E., Samonds, K.E., 2013. Stable carbon isotope values confirm a recent increase in grasslands in northwestern Madagascar. *Holocene* 23, 1066–1073.
- Crowley, B.E., Godfrey, L.R., Bankoff, R.J., Perry, G.H., Culleton, B.J., Kennett, D.J., Sutherland, M.R., Samonds, K.E., Burney, D.A., 2017. Island-wide aridity did not trigger recent megafaunal extinctions in Madagascar. *Ecography* 40, 901–912.
- Crowther, A., Lucas, L., Helm, R., Horton, M., Shipton, C., Wright, H.T., Walshaw, S., Pawlowicz, M., Radimilahy, C., Douka, K., Picornell-Gelabert, L., Fuller, D.Q., Boivin, N.L., 2016. Ancient crops provide first archaeological signature of the westward Austronesian expansion. *Proc. Natl. Acad. Sci. Unit. States Am.* 113, 6635–6640.
- Cuthbert, M.O., Baker, A., Jex, C.N., Graham, P.W., Treble, P.C., Anderson, M.S., Acworth, R.I., 2014. Drip water isotopes in semi-arid karst: implications for speleothem paleoclimatology. *Earth Planet Sci. Lett.* 395, 194–204.
- Denniston, R.F., González, L.A., Baker, R.G., Amerom, Y., Reagan, M.K., Edwards, R.L., Alexander, E.C., 1999. Speleothem evidence for Holocene fluctuations of the prairie-forest ecotone, north-central USA. *Holocene* 9, 671–676.
- Dewar, R.E., Richard, A.F., 2012. Madagascar: a history of arrivals, what happened, and will happen next. *Annu. Rev. Anthropol.* 41, 495–517.
- Dewar, R.E., Radimilahy, C., Wright, H.T., Jacobs, Z., Kelly, G.O., Berna, F., 2013. Stone tools and foraging in northern Madagascar challenge Holocene extinction models. *Proc. Natl. Acad. Sci. Unit. States Am.* 110, 12583–12588.
- De Wit, M.J., 2003. Madagascar: heads it's a continent, tails it's an island. *Annu. Rev. Earth Planet Sci.* 31, 213–248.
- Donohoe, A., Marshall, J., Ferreira, D., McGee, D., 2013. The relationship between ITCZ location and cross-equatorial atmospheric heat transport: from the seasonal cycle to the last glacial maximum. *J. Clim.* 26, 3597–3618.
- Dorale, J.A., González, L.A., Reagan, M.K., Pickett, D.A., Murrell, M.T., Baker, R.G., 1992. A high-resolution record of Holocene climate change in speleothem calcite from Cold WaterCave, northeast Iowa. *Science* 258, 1626–1630.
- Douglass, K., Zinke, J., 2015. Forging ahead by land and by sea: archaeology and paleoclimate reconstruction in Madagascar. *Afr. Archaeol. Rev.* 32, 267–299.
- Du Puy, D., Moat, J., 1996. A refined classification of the primary vegetation of Madagascar based on the underlying geology: using GIS to map its distribution and to assess its conservation status. In: Lourenco, W.R. (Ed.), *Biogeographie de Madagascar*. Éditions de l'ORSTOM, Paris, pp. 205–218 + 3 maps.
- Edwards, R.L., Chen, J.H., Wasserburg, G.J., 1987. ^{238}U , ^{234}U , ^{230}Th , ^{232}Th systematics and the precise measurement of time over the past 500,000 years. *Earth Planet Sci. Lett.* 81, 175–192.
- Field, M.S., 2002. A Lexicon of Cave and Karst Terminology with Special Reference to Environmental Karst Hydrology. United States Environmental Protection Agency Publication EPA/600/R-02/003.
- Gergis, J., Fowler, A.M., 2009. A history of ENSO events since A.D. 1525: implications for future climate change. *Climatic Change* 92, 343–387.
- Godfrey, L.R., Crowley, B.E., Samonds, K.E., Sutherland, M.R., 2015. Did climate change trigger megafaunal extinctions in Madagascar? *Am. J. Phys. Anthropol.* 156 (Suppl. 60), 147–148.
- Godfrey, L.G., Scroxton, N., Crowley, B.E., Burns, S.J., Sutherland, M.R., Pérez, V.R., Faina, P., McGee, D., Ranivoarimanana, L., 2019. A new interpretation of Madagascar's megafaunal decline: the "Subsistence Shift Hypothesis". *J. Hum. Evol.* 130, 126–140.
- Gommery, D., Ramanivosoa, B., Faure, M., Guérin, C., Kerloc'h, P., Sénégas, F., Randrianantenaina, H., 2011. Les plus anciennes traces d'activités anthropiques de Madagascar sur des ossements d'hippopotames subfossiles d'Anjohibe (Province de Mahajanga). *Comptes Rendus Palevol* 10, 271–278.
- Gunn, J., 2004. Encyclopedia of Caves and Karst Science. Fitzroy Dearborn, New York.
- Hansford, J., Wright, P.C., Rasoamiaramanana, A., Pérez, V.R., Godfrey, L.R., Erickson, D., Thompson, T., Turvey, S.T., 2018. Early Holocene human presence in Madagascar evidenced by exploitation of avian megafauna. *Sci. Adv.* 4, eaat6925.
- Hesterberg, R., Siegenthaler, U., 1991. Production and stable isotope composition of CO₂ in a soil near Bern, Switzerland. *Tellus* 43B, 197–205.
- Ingram, J.C., Dawson, T.P., 2005. Climate change impacts and vegetation response on the island of Madagascar. *Philos. Trans. Roy. Soc. Londn Ser. A-Math. Phys. Eng. Sci.* 363 (1826), 55–59.
- Jiménez de Cisneros, C., Caballero, E., 2011. Carbon isotope values as paleoclimatic indicators. Study on stalagmite from Nerja Cave, South Spain. *Carbonates Evaporites* 26, 41–46.
- Jolly, Alison, 1980. *A World like Our Own: Man and Nature in Madagascar*. Yale University Press, New Haven.
- Jury, M.R., 2003. The climate of Madagascar. In: Goodman, S.M., Benstead, J.P. (Eds.), *The Natural History of Madagascar*. University of Chicago Press, pp. 75–87.
- Jury, M.R., Pathack, B., 1991. A study of climate and weather variability over the tropical southwest Indian Ocean: Meteorol. Atmos. Phys. 47, 37–48.
- Jury, M.R., Parker, B.A., Raholjao, N., Nassor, A., 1995. Variability of summer rainfall over Madagascar: climatic determinants at interannual scales. *Int. J. Climatol.* 15 (12), 1323–1332.
- Kang, S.M., Held, I.M., Frierson, D.M.W., Zhao, M., 2008. The response of the ITCZ to extratropical thermal forcing: idealized slab-ocean experiments with a GCM. *J. Clim.* 21, 3521–3532.
- Kim, S.T., O'Neil, J.R., Hillaire-Marcel, C., Mucci, A., 2007. Oxygen isotope fractionation between synthetic aragonite and water: influence of temperature and Mg²⁺ concentration. *Geochem. Cosmochim. Acta* 71, 4704–4715.
- Kottek, M., Grieser, J., Beck, C., Rudolf, B., Rubel, F., 2006. World map of the Köppen-Geiger climate classification updated. *Meteorol. Z.* 15, 259–263.
- Lachnit, M.S., 2009. Climate and environmental controls on speleothem oxygen-isotope values. *Quat. Sci. Rev.* 28, 412–432.
- Lambert, W.J., Aharon, P., 2011. Controls on dissolved inorganic carbon and $\delta^{13}\text{C}$ in cave waters from DeSoto Caverns: implications for speleothem $\delta^{13}\text{C}$ assessments. *Geochem. Cosmochim. Acta* 75 (3), 753–768.
- Lauritzen, S.E., Lundberg, J., 1999. Speleothems and climate: a special issue of the Holocene. *Holocene* 9, 643–647.
- Leroux, M., 2001. *The Meteorology and Climate of Tropical Africa*. Springer, London and New York, p. 548.
- Liu, Y., Cai, Q.F., Song, H.M., et al., 2011. Amplitudes, rates, periodicities and causes of temperature variations in the past 2485 years and future trends over the central-eastern Tibetan Plateau. *Chin. Sci. Bull.* 56, 2986–2994. <https://doi.org/10.1007/s11434-011-4713-7>.
- MacPhee, R.D.E., Burney, D.A., 1991. Dating of modified femora of extinct dwarf hippopotamus from southern Madagascar: implications for constraining human colonization and vertebrate extinction events. *J. Archaeol. Sci.* 18, 695–706.
- Markowska, M., Baker, A., Andersen, M.S., Jex, C.N., Cuthbert, M.O., Rau, G.C., Graham, P.W., Rutledge, H., Mariethoz, G., Marjo, C.E., Treble, P.C., Edwards, N., 2016. Semiarid zone caves: evaporation and hydrological controls on $\delta^{18}\text{O}$ drip water composition and implications for speleothem paleoclimate reconstructions. *Quat. Sci. Rev.* 131, 285–301.
- Matsumoto, K., Burney, D.A., 1994. Late Holocene environments at Lake Mitsinjo, northwestern Madagascar. *Holocene* 4, 16–24.
- Mavume, A.F., Rydberg, L., Rouault, M., Lutjeharms, J.R.E., 2009. Climatology and landfall of tropical cyclones in the south-west Indian Ocean. *West. Indian Ocean J. Mar. Sci.* 8, 15–36.
- McCrea, J.M., 1950. On the isotopic chemistry of carbonates and a paleotemperature scale. *J. Chem. Phys.* 18, 849–857.
- McDermott, F., 2004. Palaeo-climate reconstruction from stable isotope variations in speleothems: a review. *Quat. Sci. Rev.* 23, 901–918.
- Middleton, J., Middleton, V., 2002. Karst and caves of Madagascar. *Cave Karst Sci.* 29, 13–20.
- Mitchell, P., 2019. Settling Madagascar: when did people first colonize the world's largest island? *J. I. Coast Archaeol.* <https://doi.org/10.1080/15564894.2019.1582567>.
- Mittermeier, R., Ganzhorn Jr., Konstant, W., Glander, K., Tattersall, I., Groves, C., Rylands, A., Hapke, A., Ratsimbazafy, J., Mayor, M., Louis, E., Rumpf, Y., Schwitzer, C., Rasoloarison, R., 2008. Lemur diversity in Madagascar. *Int. J. Primatol.* 29, 1607–1656.
- Muigg, B., Seim, A., Tegel, W., Werther, L., Herzig, F., Schmidt, J., Zielhofer, C., Land, A., Büntgen, U., 2020. Tree rings reveal dry conditions during Charlemagne's Fossa Carolina construction in 793 CE. *Quat. Sci. Rev.* 227, 106040.
- Nagovitsyn, Y.A., 2001. Solar activity during the last two millennia: solar patrol in ancient and medieval China. *Geomagn. Aeron.* 41, 680–688.
- Nassor, A., Jury, M.R., 1998. Intra-seasonal climate variability of Madagascar. Part 1: mean summer conditions. *Meteorol. Atmos. Phys.* 65, 31–41.
- Neelin, J.D., 2011. *Climate Change and Climate Modeling*. Cambridge University Press, Cambridge, p. 282.
- Nicholson, S.E., 2018. The ITCZ and the seasonal cycle over equatorial Africa. *Bull. Am. Meteorol. Soc.* 99, 337–348.
- Paul, D., Skrzypek, G., 2007. Assessment of carbonate-phosphoric acid analytical technique performed using GasBench II in continuous flow isotope ratio mass spectrometry. *Int. J. Mass Spectrom.* 262, 180–186.
- Perez, V.A., Godfrey, L., Nowak-Kemp, M., Burney, D.A., Ratsimbazafy, J., Vasey, N., 2005. Evidence of early butchery of giant lemurs in Madagascar. *J. Hum. Evol.* 49, 722–742.
- Pollini, J., 2010. Environmental degradation narratives in Madagascar: from colonial hegemonies to humanist revisionism. *Geoforum* 41, 711–722.

- Quémére, E., Amelot, X., Pierson, J., Crouau-Roy, B., Chiki, L., 2012. Genetic data suggest a natural prehuman origin of open habitats in northern Madagascar and question the deforestation narrative in this region. *Proc. Natl. Acad. Sci. Unit. States Am.* 109, 13028–13033.
- Railsback, L.B., 2018. A comparison of growth rate of late Holocene stalagmites with atmospheric precipitation and temperature, and its implications for paleoclimatology. *Quat. Sci. Rev.* 187, 94–111.
- Railsback, L.B., 2019. Past and possible future influence of the Atlantic Meridional Overturning Circulation on the climate responsible for concentration of geopolitical power and wealth in the North Atlantic region. *J. Ocean Clim.* 9, 1–8.
- Railsback, L.B., Brook, G.A., Chen, J., Kalin, R., Fleischer, C.J., 1994. Environmental controls on the petrology of a Late Holocene speleothem from Botswana with annual layers of aragonite and calcite. *J. Sediment. Res.* A64, 147–155.
- Railsback, L.B., Akers, P.D., Wang, L., Holdridge, G.A., Voarintsoa, N., 2013. Layer-bounding surfaces in stalagmites as keys to better paleoclimatological histories and chronologies. *Int. J. Speleol.* 42, 167–180.
- Railsback, L.B., Brook, G.A., Liang, F., Marais, E., Cheng, H., Edwards, R.L., 2016. A multi-proxy stalagmite record from northwestern Namibia of regional drying with increasing global-scale warmth over the last 47 kyr: the interplay of a globally shifting ITCZ with regional currents, winds, and rainfall. *Palaeogeogr. Palaeoclimatol. Palaeoecol.* 461, 109–121.
- Railsback, L.B., Brook, G.A., Liang, F., Voarintsoa, N.R.G., Cheng, H., Edwards, R.L., 2018. A multi-proxy climate record from northwestern Botswana stalagmite suggesting wetness late in the Little Ice Age (1810–1820 CE) and drying thereafter in response to changing migration of the tropical rain belt or ITCZ. *Palaeogeogr. Palaeoclimatol. Palaeoecol.* 506, 139–153.
- Raveloson, M.L.T., Newsome, D., Golonka, J., di Cencio, A., Randrianaly, H.N., 2018. The contribution of paleontology in the development of geotourism in northwestern Madagascar: a preliminary assessment. *Geoheritage* 10, 731–738.
- Richardson, P.L., 2007. Agulhas leakage into the Atlantic estimated with subsurface floats and surface drifters. *Deep-Sea Res. Part I Oceanogr. Res. Pap.* 54, 1361–1389.
- Romanek, C.S., Grossman, E.L., Morse, J.W., 1992. Carbon isotopic fractionation in synthetic aragonite and calcite: effects of temperature and precipitation rate. *Geochem. Cosmochim. Acta* 56, 419–430.
- Saji, N.H., Goswami, B.N., Vinayachandran, P.N., Yamagata, T., 1999. A dipole mode in the tropical Indian Ocean. *Nature* 401, 360–363.
- Scott, L., Holmgren, K., Talma, A.S., Woodborne, S., Vogel, J.C., 2003. Age interpretation of the wonderkrater spring sediments and vegetation change in the savanna biome, limpopo province, South Africa. *South Afr. J. Sci.* 99, 484–494.
- Scropton, N., Burns, S.J., McGee, D., Hardt, B., Godfrey, L.R., Ranivoharimanana, L., Faina, P., 2017. Hemispherically in-phase precipitation variability over the last 1700 years in a Madagascar speleothem record. *Quat. Sci. Rev.* 164, 25–36.
- Shen, C.C., Edwards, R.L., Cheng, H., Dorale, J.A., Thomas, R.B., Moran, S.B., Weinstein, S.E., Edmonds, H.N., 2002. Uranium and thorium isotopic and concentration measurements by magnetic sector inductively coupled plasma mass spectrometry. *Chem. Geol.* 185, 165–178.
- Singarayer, J.S., Valdes, P.J., Roberts, W.H.G., 2017. Ocean dominated expansion and contraction of the late Quaternary tropical rainbelt. *Sci. Rep.* 7, 9382.
- Skrypek, G., Paul, D., 2006. $\delta^{13}\text{C}$ analyses of calcium carbonate: comparison between the GasBench and elemental analyzer techniques. *Rapid Commun. Mass Spectrom.* 20, 2915–2920.
- Sletten, H.R., Railsback, L.B., Liang, F., Brook, G.A., Marais, E., Hardt, B.F., Cheng, H., Edwards, R.L., 2013. A petrographic and geochemical record of climate change over the last 4600 years from a northern Namibia stalagmite, with evidence of abruptly wetter climate at the beginning of southern Africa's Iron Age. *Palaeogeogr. Palaeoclimatol. Palaeoecol.* 376, 149–162.
- Treble, P.C., Baker, A., Ayliffe, L.K., Cohen, T.J., Hellstrom, J.C., Gagan, M.K., Frisia, S., Drysdale, R.N., Griffiths, A.D., Borsato, A., 2017. Hydroclimate of the Last Glacial Maximum and deglaciation in southern Australia's arid margin interpreted from speleothem records (23–15 ka). *Clim. Past* 13, 667–687.
- Tyson, P., 2000. *The Eighth Continent*. William Morrow, New York, p. 374.
- Virah-Sawmy, M., Willis, K.J., Gillson, L., Williams, J., 2010. Evidence for drought and forest declines during the recent megafaunal extinctions in Madagascar. *J. Biogeogr.* 37, 506–519.
- Voarintsoa, N.G., Brook, G.A., Liang, F., Marais, E., Hardt, B., Cheng, H., Edwards, R.L., Railsback, L.B., 2016. Stalagmite multi-proxy evidence of wet and dry intervals in northeastern Namibia: linkage to latitudinal shifts of the Inter-Tropical Convergence Zone and changing solar activity from AD 1400 to 1950. *Holocene* 27, 384–396.
- Voarintsoa, N.R.G., Wang, L., Railsback, L.B., Brook, G.A., Liang, F., Cheng, H., Edwards, R.L., 2017a. Multiple proxy analyses of a U/Th-dated stalagmite to reconstruct paleoenvironmental changes in northwestern Madagascar between 370CE and 1300CE. *Palaeogeogr. Palaeoclimatol. Palaeoecol.* 469, 138–155.
- Voarintsoa, N.R.G., Railsback, L.B., Brook, G.A., Wang, L., Kathayat, G., Cheng, H., Li, X., Edwards, R.L., Rakotondrazafy, A.F.M., Razanatseheno, M.O.M., 2017b. Three distinct Holocene intervals of stalagmite deposition and nondeposition revealed in NW Madagascar, and their paleoclimate implications. *Clim. Past* 13, 1771–1790.
- Voarintsoa, N.R.G., Matero, I.S.O., Railsback, L.B., Gregoire, L.J., Thindall, J., Sime, L., Cheng, H., Edwards, R.L., Brook, G.A., Kathayat, G., Li, X., Rakotondrazafy, A.F.M., Razanatseheno, M.O.M., 2019. Investigating the 8.2 ka event in northwestern Madagascar: insight from data-model comparisons. *Quat. Sci. Rev.* 204, 172–186.
- von Cabanis, Y., Chabouis, L., Chabouis, F., 1969. *Végétaux et Groupements végétaux de Madagascar I. Tananarive*. Bureau pour le Développement de la Production Agricole.
- Waliser, D.E., Gautier, C., 1993. A satellite-derived climatology of the ITCZ. *J. Clim.* 6, 2162–2174.
- Wang, L., Brook, G.A., Burney, D.A., Voarintsoa, N.R.G., Liang, F., Cheng, H., Edwards, R.L., 2019. The African Humid Period, rapid climate change events, the timing of human colonization, and megafaunal extinctions in Madagascar during the Holocene: evidence from a 2m Anjohibe Cave stalagmite. *Quat. Sci. Rev.* 210, 136–153.
- Webster, P.J., Moore, A.M., Loschnigg, J.P., Leben, R.R., 1999. Coupled ocean-atmosphere dynamics in the Indian Ocean during 1997–98. *Nature* 401, 356–360.
- World Meteorological Organization, 2014. *El Niño – Southern Oscillation*, vol. 1145. WMO, p. 8.
- Wright, H.T., Rakotoarisoa, J.A., Heurtebize, G., Vérin, P., 1993. The evolution of settlement systems in the Efaho River Valley, Anosy: a preliminary report on the archaeological reconnaissances of 1983–1986. *Bull. Indo-Pacific Prehis. Assoc.* 13, 61–93.
- Wright, H.T., Vérin, P., Ramilisonina Burney, D., Burney, L.P., Matsumoto, K., 1996. The evolution of settlement systems in the bay of Boeny and the mahavavy river valley, north-western Madagascar. *XXXI Azania* 37–73.
- Yoder, A.D., Nowak, M.D., 2006. Has vicariance or dispersal been the predominant biogeographic force in Madagascar? Only time will tell. *2006 Annu. Rev. Ecol. Evol. Syst.* 37, 405–431.
- Zhang, Y., Du, Y., Qu, T., 2016. A sea surface salinity dipole mode in the tropical Indian Ocean. *Clim. Dynam.* 47, 2573–2585.
- Zhu, X., Zhang, M., Lin, Y., Qin, J., Yang, Y., 2006. Carbon isotopic records from stalagmites and the signification of paleo-ecological environment in the area of Guangxi–Guizhou, China. *Environ. Geol.* 51, 267–273.
- Ziegler, M., Simon, M.H., Hall, I.R., Barker, S., Stringer, C., Zahn, R., 2013. Development of Middle Stone Age innovation linked to rapid climate change. *Nat. Commun.* 4, 1905.
- Zinke, J., Dullo, W.C., Heiss, G.A., Eisenhauer, A., 2004. ENSO and Indian Ocean subtropical dipole variability is recorded in a coral record off southwest Madagascar for the period 1659 to 1995. *Earth Planet Sci. Lett.* 228, 177–194.